



ELSEVIER

Available online at www.sciencedirect.com



Journal of Theoretical Biology ■ (■■■) ■■■-■■■

**Journal of
Theoretical
Biology**

www.elsevier.com/locate/yjtbi

An old paper revisited: “A mathematical model of carbohydrate energy metabolism. Interaction between glycolysis, the Krebs cycle and the H-transporting shuttles at varying ATPases load” by V.V. Dynn timer, R. Heinrich and E.E. Sel’kov

Christine Nazaret^a, Jean-Pierre Mazat^{b,*}

^aIMB, Université de Bordeaux 2, 146 Rue Léo-Saignat, F 33076 Bordeaux-cedex, France
^bInserm U688, Université de Bordeaux 2, 146 Rue Léo-Saignat, F 33076 Bordeaux-cedex, France

Received 15 June 2007; received in revised form 21 December 2007; accepted 7 January 2008

Abstract

We revisit an old Russian paper by V.V. Dynn timer, R. Heinrich and E.E. Sel’kov (1980) describing: “A mathematical model of carbohydrate energy metabolism. Interaction between glycolysis, the Krebs cycle and the H-transporting shuttles at varying ATPases load”. We analyse the model mathematically and calculate the control coefficients as a function of ATPase loads. We also evaluate the structure of the metabolic network in terms of elementary flux modes.

We show how this model can respond to an ATPase load as well as to the glucose supply. We also show how this simple model can help in understanding the articulation between the major blocks of energetic metabolism, i.e. glycolysis, the Krebs cycle and the H-transporting shuttles.

© 2008 Published by Elsevier Ltd.

Keywords: Energetic metabolism; Elementary flux mode; Control coefficient; Regulation by branched structure

1. Introduction

Two years ago, we offered an Erasmus student of Reinhart Heinrich to study a simplified model of the TCA cycle during her stay in Bordeaux. Reinhart told one of us (J.P.M.) that he had developed a simple model of the TCA cycle during his stay in Pushchino with E. Sel’kov and V. Dynn timer (Dynn timer *et al.*, 1980a, b and the letter, Fig. 1 in Supplementary Materials). In fact, his papers involved not only a simplified version of the Krebs cycle but also a simplification of glycolysis and of the H-transporting shuttles.

Abbreviations: GAP, glyceraldehyde-3-phosphate; DAP, dihydroxyacetone phosphate; 1, 3-DPG, 1, 3 DPG, 1, 3 diphosphoglycerate; α -GP, α -glycerolphosphate.

*Corresponding author. Tel.: +33 557 571 379; fax: +33 557 571 612.

E-mail addresses: nazaret@sm.u-bordeaux2.fr (C. Nazaret), jpm@u-bordeaux2.fr (J.-P. Mazat).

In this paper, we present the model developed by Dynn timer, Heinrich and Sel’kov in the first paper (1980) and interpret the results in terms of the variations of the control coefficients depending on the ATPase load. We also describe the elementary modes of the system, a concept which was not developed at that time.

2. Presentation of the model

Fig. 1 depicts the metabolic network involving glycolysis, the Krebs cycle, oxidative phosphorylation, ATP consumption and the glycerolphosphate shuttle. It reproduces the original Fig. 1 in the Russian paper with slight modifications indicated below.

Glycolysis is reduced to three reactions (reactions 1, 3 and 5): reaction 1 describes the conversion from glucose to glyceraldehyde-3-phosphate (GAP) which consumes two ATP and produces two GAP; reaction 3 contains the GAP dehydrogenase reaction that produces NADH in the

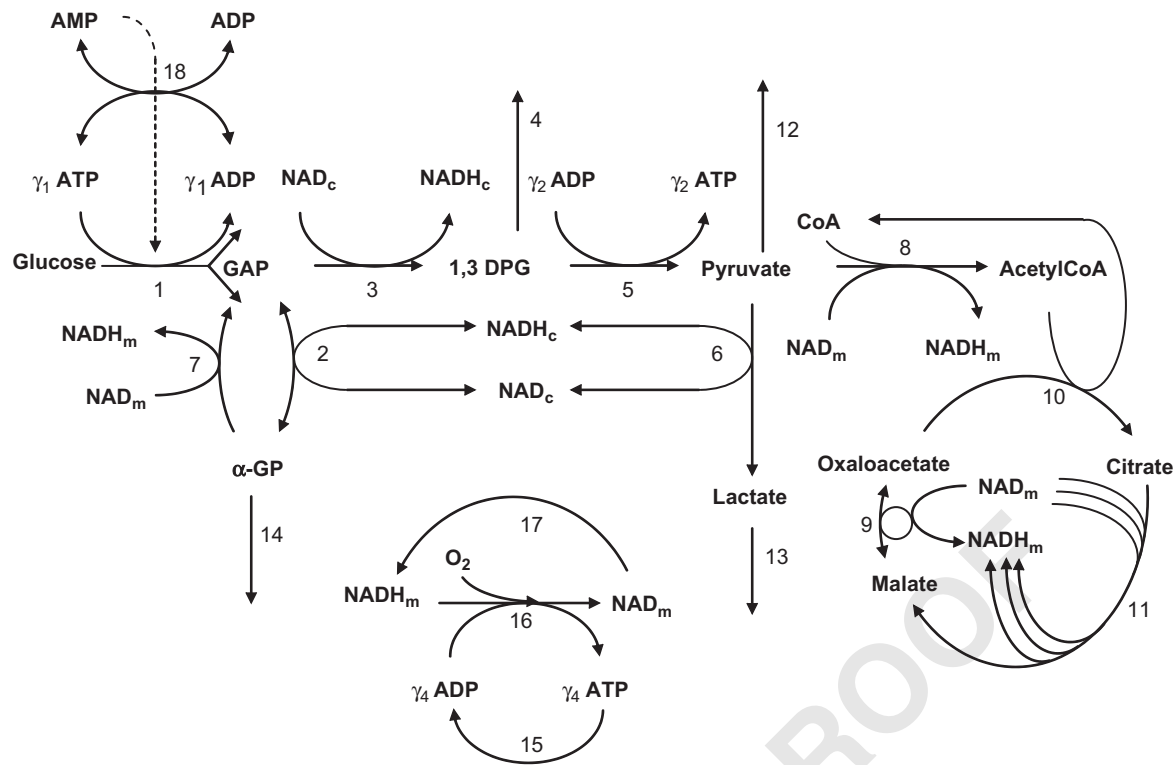


Fig. 1. Kinetic model of carbohydrate energy metabolism. 1, 3, 5 and 6: Glycolytic reactions; 2 and 7: cytoplasmic and mitochondrial α -glycerophosphate reactions of H-transporter; 8: pyruvate dehydrogenase; 9, 10 and 11: Krebs cycle; 4, 12, 13 and 14: glycolytic intermediates and α -glycerophosphate efflux; 15: total ATPase reactions; 16: oxidative phosphorylation; 17: NADH dehydrogenase; 18: adenylate kinase; dotted line: PFK activation by AMP; the indexes *c* and *m* correspond to the cytoplasmic and mitochondrial compartments. $\gamma_1 = \gamma_2 = 2$; $\gamma_3 = 3$ for NAD_m in Krebs cycle; $\gamma_4 = 3$ ATP for one NADH_m .

cytosol (NADH_c) and 1,3-diphosphoglycerate (1,3-DPG); reaction 5 lumps together the remaining glycolysis reactions which produces two ATP molecules per GAP (four per glucose molecule) and one molecule of pyruvate (two per glucose molecule). Pyruvate can exit, be used for another metabolic pathway (reaction 12) or be converted to lactate (reactions 6) with the simultaneous reoxidation of NADH_c . Lactate and 1,3-DPG can also escape from the metabolic network (reactions 13 and 4, respectively).

Reaction 8 is the pyruvate dehydrogenase reaction with the production of one NADH_m molecule in mitochondria. Krebs cycle is summarized in three reactions (reactions 9–11) producing four molecules of NADH_m . In this model, FADH_2 is not taken into account and replaced when necessary, as in the Krebs cycle, by a NADH molecule. The production of ATP (or GTP) by the Krebs cycle is ignored.

The conversion of NADH_c to NADH_m is described by the glycerolphosphate shuttle (reactions 2 and 7), where once again the FADH_2 involved in this shuttle is replaced by NADH_m . The malate–aspartate shuttle is not taken into account.

Finally, oxidative phosphorylation is summarized in reactions 16. Reaction 15 ensures the consumption of ATP produced by glycolysis and oxidative phosphorylation.

The irreversible reaction 17 summarizes other dehydrogenases producing NADH_m . The orientation of this reaction is changed in comparison to the original Fig. 1

of the paper. We indicate the direction from NAD_m to NADH_m in accordance with the v_{17} rate equation ($v_{17} = \beta_{17}n_1$). This is also in accordance with the differential equation (Eq. (11) of the Dynnik paper) expressing the variation of n_2 (NADH_m) where v_{17} has the same “+” sign as v_{11} , which expresses NADH_m production.

The only regulation introduced in this model is the allosteric regulation of reaction v_1 (in reality phosphofructokinase) by AMP.

At steady state, the flux through reaction 1 (v_1) represents the entry of glucose in the system. The flux through reaction 2 or 7 (v_2 or v_7) is the glycerol-3-P shuttle. The flux through reaction 5 (v_5) is the total glycolytic flux which splits in anaerobic glycolysis (v_6), and aerobic glycolysis or the Krebs cycle (v_8 , v_9 , v_{10} or v_{11} which are equal, see below). Finally, v_{16} represents the respiratory chain.

We reproduce below the equations on which the system is based.

3. Equations of the model

The variables and the time are scaled according to (Eqs. (2)–(8) and Eq. (10) in the original paper):

$$a_1 = \frac{\text{AMP}}{A_0}, \quad a_2 = \frac{\text{ADP}}{A_0}, \quad a_3 = \frac{\text{ATP}}{A_0},$$

$$r_1 = \frac{\text{NAD}_c}{N_c}, \quad r_2 = \frac{\text{NADH}_c}{N_c},$$

$$c_1 = \frac{\text{CoA}}{C_0}, \quad c_2 = \frac{\text{CoASAc}}{C_0},$$

$$n_1 = \frac{\text{NAD}_m}{N_m}, \quad n_2 = \frac{\text{NADH}_m}{N_m},$$

$$i_1 = \frac{\text{Oxa}}{I_0}, \quad i_2 = \frac{\text{Mal}}{I_0}, \quad i_3 = \frac{\text{Cit}}{I_0},$$

$$s_1 = \frac{\text{GAP}}{S_1}, \quad s_2 = \frac{\text{aGP}}{S_2}, \quad s_3 = \frac{\text{1.3DPG}}{S_3}, \quad s_4 = \frac{\text{Pyr}}{S_4}, \quad s_5 = \frac{\text{Lac}}{S_5},$$

$$\tau = t \frac{V_1^{\max}}{R_1 S_1},$$

with: $\text{AMP} + \text{ADP} + \text{ATP} = A_0$, $\text{NAD}_c + \text{NADH}_c = N_c$, $\text{CoA} + \text{CoASAc} = C_0$, $\text{NAD}_m + \text{NADH}_m = N_m$ and $\text{Oxa} + \text{Mal} + \text{Cit} = I_0$ ($i_1 + i_2 + i_3 = 1$).

S_1, S_2, S_3, S_4 and S_5 are the concentrations of the substrates of reactions 2, 3, 4, 5 and 6, respectively, for which $v = V_M/2$.

R_1 is defined through the pool $X = \text{GAP} + \text{DAP} + \text{F-1,6-P}_2$, i.e. the pool of potential C_3 sugars.

Eqs. (1) in the original paper show that $X = (1 + K_1^\circ)(1 + 2[\text{GAP}/K_2^\circ])[\text{GAP}] \cong (1 + 2K_1^\circ)[\text{GAP}] = R_1[\text{GAP}]$, where K_1° and K_2° are the equilibrium constants of triosephosphate isomerase and aldolase, respectively.

With these new scaled variables, the rate equations read (Eqs. (9) of the original paper):

$$v_1 = \frac{a_3}{a_3 + \mu_1} \frac{a_1/\mu_0 + \omega}{a_1/\mu_0 + 1},$$

$$v_2 = \beta_2(s_1 r_2 - \delta_2 s_2 r_1),$$

$$v_3 = \beta_3(s_1 r_1 - \delta_3 s_3 r_2), \quad v_4 = \beta_4 s_3, \quad v_5 = \beta_5 s_3 a_2,$$

$$v_6 = \beta_6(s_4 r_2 - \delta_6 s_5 r_1), \quad v_7 = \beta_7 s_2 n_1, \quad v_8 = \beta_8 s_4 c_1 n_1,$$

$$v_9 = \beta_9(i_2 n_1 - \delta_9 i_1 n_2), \quad v_{10} = \beta_{10} i_1 c_2, \quad v_{11} = \beta_{11} i_3 n_1,$$

$$v_{12} = \beta_{12} s_4, \quad v_{13} = \beta_{13} s_5, \quad v_{14} = \beta_{14} s_2,$$

$$v_{15} = \beta_{15} \frac{a_3}{a_3 + \mu_{15}},$$

$$v_{16} = \beta_{16} \frac{n_2}{n_2 + \mu'_{16}} \frac{a_2}{a_2 + \mu_{16}}, \quad v_{17} = \beta_{17} n_1,$$

$$v_{18} = \beta_{18}(a_1 a_3 - \delta_{18} a_2 a_2),$$

where the β_i ($i = 2-18$) are the normalized rate constants, assuming that the corresponding β_1 of the first reaction is equal to 1. δ_i ($i = 2, 3, 6, 9$ and 18) involve the equilibrium constant of the reaction. μ_{15}, μ_{16} and μ'_{16} involve the Km for ATP, ADP and NADH_m . μ_0 and $\omega \ll 1$ are activation constants for AMP activation.

The differential equations expressing the variations of the scaled variables are (Eq. (11) of the original paper):

$$\frac{ds_1}{d\tau} = 2v_1 - v_2 - v_3 + v_7,$$

$$\varepsilon_1 \frac{ds_2}{d\tau} = v_2 - v_7 - v_{14},$$

$$\varepsilon_2 \frac{ds_3}{d\tau} = v_3 - v_4 - v_5,$$

$$\varepsilon_3 \frac{ds_4}{d\tau} = v_5 - v_6 - v_8 - v_{12},$$

$$\varepsilon_4 \frac{ds_5}{d\tau} = v_6 - v_{13},$$

$$\varepsilon_5 \frac{da_3}{d\tau} = 2v_5 - 2v_1 + 3v_{16} - v_{15} - v_{18},$$

$$\varepsilon_5 \frac{da_1}{d\tau} = -v_{18},$$

$$\varepsilon_6 \frac{dr_1}{d\tau} = v_6 + v_2 - v_3,$$

$$\varepsilon_7 \frac{dn_2}{d\tau} = 3v_{11} + v_8 + v_7 + v_9 + v_{17} - v_{16},$$

$$\varepsilon_8 \frac{di_1}{d\tau} = v_9 - v_{10},$$

$$\varepsilon_8 \frac{di_2}{d\tau} = v_{11} - v_9,$$

$$\varepsilon_9 \frac{dc_2}{d\tau} = v_8 - v_{10},$$

$$a_2 = 1 - a_1 - a_3, \quad r_2 = 1 - r_1, \quad n_1 = 1 - n_2,$$

$$c_1 = 1 - c_2, \quad i_3 = 1 - i_1 - i_2.$$

Glucose, phosphate and oxygen are assumed to be in excess, i.e. they are considered as external variables.

We are able to demonstrate that for each set of positive initial conditions (metabolite concentrations), the system possesses a unique solution globally defined on $[0, +\infty)$. All metabolite concentrations remain positive for all $t > 0$. Although we are not able to prove analytically that a unique steady state exists, the concentrations converge, at least numerically, towards a single limiting value which is an indication of the existence of a unique steady state. No oscillatory behaviour has been observed in our simulations. Details of the proof can be found in the Supplementary Material.

Figs. 2 and 3 are drawn with these equations and are at least qualitatively equivalent with the same figures of the original paper. They confirm the conclusions of the original work, i.e. that the ATP concentration is stable and high (around 0.8–1), at least until $\beta_{15} \leq 10$. In these conditions, the ADP concentration is low and the AMP is close to zero (Fig. 2a and 3a). When β_{15} varies from 1 to 10, the rates of glucose consumption (v_1) and of the Krebs cycle (v_{10}) increase by a factor of 8 and 11, respectively, similar to the increase in β_{15} by a factor of 10 (Fig. 3c). There is a lower increase ($5 \times$) in the NADH shuttle (v_2 or v_7), showing that the increase in ATP production is split between glycolysis and oxidative phosphorylation. Due to the increase in glucose production, there is an increase in pyruvate, but not all the pyruvate molecules enter the Krebs cycle; some are metabolized in the lactate-regenerating part of the

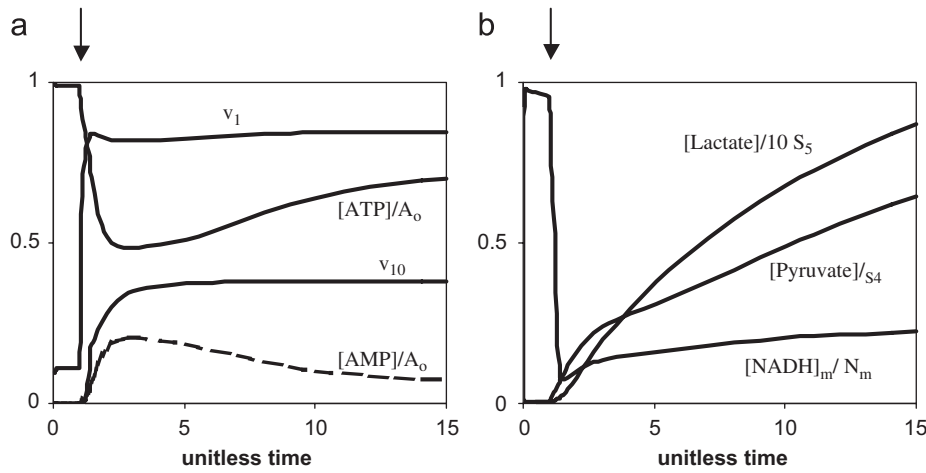


Fig. 2. Metabolism transfer to new steady state under increased ATPase load (v_{15}) at time indicated by the arrow. v_1 , v_{10} , unitless rates of glycolysis and Krebs cycle; t , unitless time. Curves are drawn by numerical integration of the model with: $\mu_0 = 0.003$; $\mu_i = 0.1$ ($i = 1, 15, 16$); $\mu'_{16} = 0.1$; $\omega = 0.1$; $\delta_2 = 0.1$; $\delta_3 = 25$; $\delta_6 = 0.003$; $\delta_9 = 25$; $\delta_{18} = 1$; $\varepsilon_i = 1$ ($i = 1, \dots, 4$); $\varepsilon_5 = 4$; $\varepsilon_6 = 0.2$; $\varepsilon_7 = 0.2$; $\varepsilon_8 = 0.2$; $\varepsilon_9 = 0.2$; $\beta_2 = 10$; $\beta_3 = 10$; $\beta_4 = 0.01$; $\beta_5 = 10$; $\beta_6 = 200$; $\beta_7 = 25$; $\beta_8 = 3$; $\beta_9 = 100$; $\beta_{10} = 5$; $\beta_{11} = 3$; $\beta_{12} = 0.1$; $\beta_{13} = 0.1$; $\beta_{14} = 0.5$; $\beta_{16} = 5$; $\beta_{17} = 0.01$; $\beta_{18} = 100$; $\beta_{15} = 1$ before the ATPase activity is increased and $\beta_{15} = 10$ after this increase.

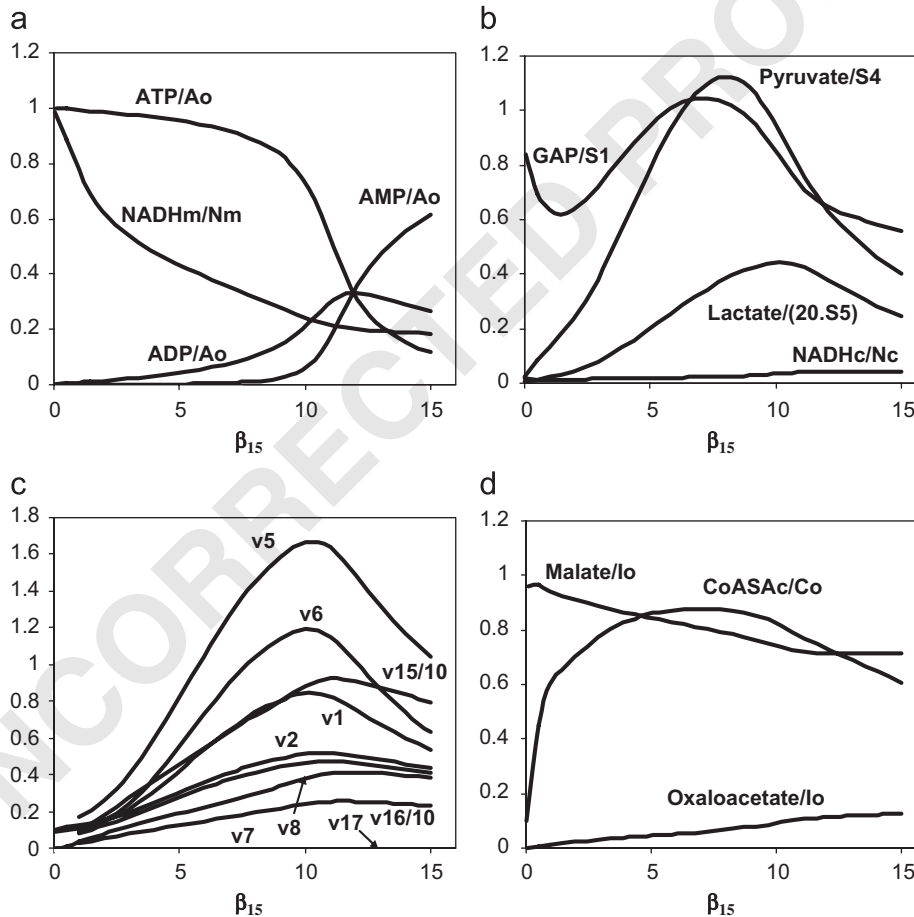


Fig. 3. Dependence of steady-state values of the variables and relative rates of glycolysis (v_1), H-transporter through the glycerol-3P-shuttle (v_2 and v_7), total glycolytic flux (v_5), anaerobic glycolysis (v_6), Krebs cycle (v_8), ATP consumption (v_{15}) and respiratory chain (v_{16}) on ATPase load (β_{15}) in the model. The rate values v_{15} and v_{16} are divided by 10 for clarity. Parameters as in Figs. 1 and 2.

NAD_c which is necessary for glycolysis (Figs. 2b and 3b). The pyruvate molecules entering the Krebs cycle lead to an increase in acetylCoA concentration. However, the con-

centrations of oxaloacetate and malate remain more or less constant so the increase in the flux through the Krebs cycle is mainly due to the increase in acetylCoA concentration

(note that reaction 9 is at equilibrium with $\beta_9=100$). On the contrary, when β_{15} exceeds the value of 10, the consumption of ATP (v_{15}) exceeds the regeneration possibilities of the system, so the ATP concentration dramatically decreases (Fig. 3a). Since the first steps of glycolysis are lumped together in v_1 and are sensitive to the ATP concentration, v_1 decreases when the ATP concentration decreases, thus reinforcing the effect of the ATP concentration decrease. This leads to a decrease in nearly all metabolite concentrations and fluxes at the steady state (see Figs. 2 and 3). It should be noted that the positive regulation by AMP, which operates at $\beta_{15}<10$, cannot compensate for the negative effect of the ATP decrease. In fact, at high AMP concentration, the v_1 equation simplifies to $v_1 = a_3/(a_3 + \mu_1)$, irrespective of AMP concentration.

These coordinated changes at different steady states between the three parts of the metabolic network (glycolysis, Krebs cycle and H-transporting shuttle) are also well evidenced in view of the flux control coefficients.

4. Control coefficients

In the summary of the paper, the authors state that an increase in ATPase load leads to a rise in glucose consumption. As mentioned above, this is true for β_{15} changing from 1 to 10. It is clear from Table 1 that all rates increase when β_{15} changes from 1 to 10. The yield in ATP synthesis per glucose consumed (v_{15}/v_1) is quite constant (around a value of 10) in this β_{15} range. However, it should be noted that the yield increases ($v_{15}/v_1 = 15$ for β_{15}) when v_{15} and v_1 decrease. As noted by the authors, in this β_{15} range (1–10), the glycolysis and Krebs cycle rates are increased approximately by a factor of 10, and the leaks either increase to a lesser extent (v_{12} , v_{14}) or decrease (v_4). This is not the case for v_{13} which is increased by a factor 12 due to its role in regenerating NAD_c for glycolysis. The values in Table 2(A and B) summarize the control coefficients of all the flux through each reaction towards each rate function. The control coefficient (logarithmic definition) of flux through reaction R_i is calculated by varying each rate v_j by 0.1%, and is designated as $CF_{v_j}^i$.

The highest control coefficients concern the effect of v_1 (glucose entry) and v_{15} (ATP consumption), and are similar

at both low and high ATPase load (see Table 2). The main effects of v_1 are on v_1 itself, v_3-v_6 (i.e. the flux through the glycolysis and the 1,3-DPG leak) and the leaks through $v_{12}-v_{14}$. The leaks themselves (v_4 , v_{12} , v_{14}) have control coefficients around 1 on their own flux and in some cases they have a highly negative control coefficient on the flux with which they form a branch (v_5 , v_{13}). In all cases ($\beta_{15} = 1$ or 10), the flux through the Krebs cycle is highly sensitive to variations in ATPase load.

Fig. 4 represents the continuous variation of some control coefficients towards v_{15} when β_{15} varies continuously from 1 to 15. All control coefficients in Fig. 4, except $CF_{v_{15}}^{17}$, have a negative value for $\beta_{15}>10-11$ in accordance with the negative effect of an increase in ATP consumption in this region. For β_{15} between 1 and 10, some of the control coefficients are constant around 1, such as $CF_{v_{15}}^{16}$, meaning that the respiratory rate exactly follows the ATP demand. Some others pass by a maximum largely above 1, for β_{15} around 4–5. Such is the case for $CF_{v_{15}}^1$ and $CF_{v_{15}}^5$ which are related to the glycolytic flux part of the network. This means that glycolysis becomes very sensitive to variations in ATP demand when β_{15} is around 4–5. For these values of β_{15} , the ATP concentration is nearly constant, but the AMP concentration increases and stimulates v_1 . For higher β_{15} values, the ATP concentration decreases, but there is no further activation of v_1 by AMP to compensate the activity decrease due to the decrease in ATP concentration as discussed above.

We also investigated the value of control coefficients at various ratios between the important branches of the network. With $\beta_{15} = 5$, we vary β_3/β_2 which represents the glycolysis/glycerol-P shuttle ratio, and β_8/β_6 which represents the aerobic/anaerobic glycolytic flux around the values given in the Dynnik et al. paper (10/20 and 3/200, respectively). No large variations in the control coefficients towards v_{15} , v_3 or v_8 were evidenced (not shown).

5. Elementary modes

The concept of elementary mode was not developed at the time of the original paper. The elementary flux modes (efm) represent the entire minimal pathway in a metabolic network (Schuster and Hilgetag, 1994; Schuster et al., 1999,

Table 1

Flux through the different reactions (R_1-R_{17}) at the steady states obtained for $\beta_{15}=1, 5, 10$ and 15

	R_1	R_2	R_3	R_4	R_5	R_6	R_7	R_8	R_9	R_{10}	R_{11}	R_{12}	R_{13}	R_{14}	R_{15}	R_{16}	R_{17}	Yield	R_3/R_2	R_8/R_6	R_{17}/R_{16}
Flux at $\beta_{15}=1$	0.1	0.09	0.19	0.03	0.17	0.1	0.08	0.03	0.03	0.03	0.03	0.03	0.1	0.01	0.91	0.26	0.00	9.10	2.11	0.30	0.01
Flux at $\beta_{15}=5$	0.42	0.29	0.84	0.02	0.82	0.55	0.28	0.19	0.19	0.19	0.19	0.08	0.55	0.01	4.53	1.25	0.01	10.71	2.91	0.35	0.00
Flux at $\beta_{15}=10$	0.84	0.48	1.67	0.01	1.66	1.19	0.47	0.38	0.38	0.38	0.38	0.09	1.19	0.01	8.8	2.38	0.01	10.48	3.48	0.32	0.00
Flux at $\beta_{15}=15$	0.53	0.42	1.05	0.00	1.04	0.63	0.41	0.38	0.38	0.38	0.38	0.04	0.63	0.01	7.95	2.31	0.01	15.07	2.51	0.60	0.00
Flux 5/Flux 1	4.23	3.19	4.40	0.61	4.81	5.48	3.47	6.41	6.41	6.41	6.41	2.55	5.48	0.97	4.97	4.79	2.98				
Flux 10/Flux 1	8.40	5.33	8.79	0.33	9.76	11.90	5.88	12.67	12.67	12.67	12.67	3.00	11.90	1.00	9.67	9.15	5.19				
Flux 15/Flux 1	5.28	4.64	5.50	0.13	6.13	6.28	5.09	12.61	12.61	12.61	12.61	1.17	6.28	0.99	8.74	8.88	4.29				

The yield in ATP production (v_{15}/v_1) is indicated at the end of each row. The second part of the table depicts the flux ratios of each steady state for $\beta_{15}=5, 10$ and 15 towards the first steady states $\beta_{15}=1$ considered as the reference: Flux i /Flux 1 means flux at steady state $\beta_{15}=i$ towards the corresponding flux at $\beta_{15}=1$.

Table 2
Control coefficients of the flux at steady state

	v_1	v_2	v_3	v_4	v_5	v_6	v_7	v_8	v_9	v_{10}	v_{11}	v_{12}	v_{13}	v_{14}	v_{15}	v_{16}	v_{17}	Sum	
(A)																			
Flux	0.101	0.091	0.194	0.027	0.167	0.103	0.082	0.035	0.035	0.035	0.035	0.029	0.103	0.009	0.909	0.259	0.002		
CF_1	0.96	0.00	0.00	0.01	-0.01	0.00	0.00	0.00	0.00	0.00	0.00	0.00	0.00	0.00	0.23	-0.19	0.00	1.00	
CF_2	0.61	0.08	0.00	0.15	-0.25	-0.03	0.02	0.00	0.00	-0.01	0.00	0.19	-0.16	-0.01	0.27	0.13	0.00	1.00	
CF_3	0.96	0.00	0.00	0.01	0.00	0.00	0.03	0.00	0.00	-0.02	0.00	-0.01	0.02	-0.03	0.28	-0.20	0.00	1.05	
CF_4	1.10	-0.01	0.00	0.82	-0.81	0.00	0.05	-0.01	0.00	-0.02	0.00	-0.01	0.01	-0.05	-0.70	0.62	0.00	1.00	
CF_5	0.93	-0.01	0.00	-0.12	0.13	0.00	0.03	-0.01	0.00	-0.02	0.00	-0.01	0.01	-0.03	0.44	-0.34	0.00	1.00	
CF_6	1.26	-0.08	0.00	-0.12	0.22	0.03	0.04	-0.01	0.00	-0.04	0.00	-0.18	0.16	-0.06	0.28	-0.50	0.00	0.99	
CF_7	0.55	0.07	0.00	0.16	-0.25	-0.02	0.11	-0.02	0.00	-0.07	0.00	0.19	-0.15	-0.10	0.38	0.14	0.00	1.00	
CF_8	-0.47	-0.03	0.00	0.01	0.03	0.01	-0.07	0.01	0.00	0.05	0.00	-0.08	0.06	0.07	1.35	0.07	-0.01	1.00	
CF_9	-0.47	-0.03	0.00	0.01	0.03	0.01	-0.07	0.02	0.00	0.05	0.00	-0.08	0.06	0.07	1.35	0.07	-0.01	1.02	
CF_{10}	-0.47	-0.03	0.00	0.01	0.03	0.01	-0.07	0.01	0.00	0.05	0.00	-0.08	0.06	0.07	1.35	0.07	-0.01	1.00	
CF_{11}	-0.47	-0.03	0.00	0.01	0.03	0.01	-0.07	0.01	0.00	0.05	0.00	-0.08	0.06	0.07	1.35	0.07	-0.01	1.00	
CF_{12}	1.46	0.30	-0.01	-0.28	-0.05	-0.10	0.12	-0.02	0.00	-0.08	-0.01	0.71	-0.59	-0.06	-0.12	-0.26	0.00	1.00	
CF_{13}	1.26	-0.08	0.00	-0.12	0.22	0.03	0.04	-0.01	0.00	-0.04	0.00	-0.18	0.17	-0.05	0.28	-0.50	0.00	1.00	
CF_{14}	1.20	0.15	0.00	0.10	-0.28	-0.05	-0.81	0.14	0.00	0.52	0.03	0.21	-0.30	0.84	-0.79	0.04	0.00	1.00	
CF_{15}	0.00	0.00	0.00	0.00	0.00	0.00	0.00	0.00	0.00	0.00	0.00	0.00	0.00	0.00	1.00	0.00	0.00	1.00	
CF_{16}	-0.15	0.00	0.00	0.06	-0.06	0.00	-0.01	0.00	0.00	0.01	0.00	0.00	-0.01	0.01	1.04	0.10	0.00	1.00	
CF_{17}	-0.65	-0.08	0.00	0.05	0.03	0.03	-0.08	-0.16	0.00	-0.58	-0.04	-0.02	0.15	0.07	1.17	0.11	0.99	1.00	
(B)																			
Flux	0.842	0.479	1.672	0.008	1.664	1.193	0.467	0.382	0.382	0.382	0.382	0.089	1.193	0.012	8.795	2.384	0.008		
CF_1	0.95	0.00	0.00	0.00	0.00	0.00	0.00	-0.01	0.00	-0.02	0.00	0.00	0.01	0.00	0.18	-0.11	0.00	1.00	
CF_2	0.24	0.08	-0.01	0.01	-0.08	-0.02	0.00	0.02	0.00	0.07	0.01	0.14	-0.13	0.00	0.39	0.29	0.00	1.00	
CF_3	0.96	0.00	0.00	0.00	0.00	0.00	0.01	-0.01	0.00	-0.03	-0.01	0.00	0.01	-0.01	0.19	-0.11	0.00	1.00	
CF_4	1.98	0.06	-0.01	0.99	-1.04	-0.02	0.03	0.12	0.00	0.50	0.10	0.01	-0.10	-0.02	-3.84	2.25	0.00	1.00	
CF_5	0.95	0.00	0.00	0.00	0.01	0.00	0.01	-0.01	0.00	-0.03	-0.01	0.00	0.01	-0.01	0.21	-0.12	0.00	1.00	
CF_6	1.24	-0.04	0.01	0.00	0.04	0.01	0.01	-0.01	0.00	-0.06	-0.01	-0.06	0.06	-0.01	0.11	-0.28	0.00	1.00	
CF_7	0.23	0.08	-0.01	0.01	-0.08	-0.02	0.03	0.01	0.00	0.06	0.01	0.14	-0.13	-0.02	0.40	0.29	0.00	1.00	
CF_8	-0.23	-0.01	0.00	0.00	0.01	0.00	-0.01	0.01	0.00	0.04	0.01	-0.03	0.02	0.01	1.00	0.18	0.00	1.00	
CF_9	-0.23	-0.01	0.00	0.00	0.01	0.00	-0.01	0.01	0.00	0.04	0.01	-0.03	0.02	0.01	1.00	0.18	0.00	1.00	
CF_{10}	-0.23	-0.01	0.00	0.00	0.01	0.00	-0.01	0.01	0.00	0.04	0.01	-0.03	0.02	0.01	1.00	0.18	0.00	1.00	
CF_{11}	-0.23	-0.01	0.00	0.00	0.01	0.00	-0.01	0.01	0.00	0.04	0.01	-0.03	0.02	0.01	1.00	0.18	0.00	1.00	
CF_{12}	2.11	0.47	-0.08	-0.02	-0.40	-0.13	0.04	0.03	0.00	0.12	0.02	0.87	-0.77	-0.02	-1.86	0.59	0.00	1.00	
CF_{13}	1.24	-0.04	0.01	0.00	0.04	0.01	0.01	-0.02	0.00	-0.06	-0.01	-0.06	0.06	-0.01	0.11	-0.28	0.00	1.00	
CF_{14}	0.43	0.11	-0.02	0.01	-0.11	-0.03	-0.97	0.07	0.00	0.29	0.06	0.14	-0.18	0.97	-0.05	0.26	0.00	1.00	
CF_{15}	0.06	0.00	0.00	0.00	0.00	0.00	0.00	0.01	0.00	0.03	0.01	0.00	-0.01	0.00	0.76	0.14	0.00	1.00	
CF_{16}	-0.14	0.01	0.00	0.00	-0.01	0.00	0.00	0.01	0.00	0.05	0.01	0.00	-0.01	0.00	0.88	0.20	0.00	1.00	
CF_{17}	-0.20	-0.03	0.00	0.00	0.03	0.01	-0.01	-0.05	0.00	-0.23	-0.05	0.00	0.05	0.00	0.45	0.03	1.00	1.00	

CF_i in row indicates the control coefficients of the flux through the reaction i by the rate v_j in column. A: $\beta_{15}=1$; B: $\beta_{15}=10$. The substantial values of control coefficient (between 0.25 and 0.7) are represented in bold digits; the highest are represented by bold italic numbers.

2000). The elementary modes of the system were analysed with METATOOL (Pfeiffer et al., 1999) and 11 elementary modes were found in this network (they are shown in the annexes). In addition, METATOOL gives interesting structural information on the metabolic network:

1. The v_{18} rate (adenylate kinase) is not involved in the elementary modes, indicating that it should be zero at steady state. This result is obvious if we consider the differential equation: $\varepsilon_5(da_1/dt) = -v_{18}$ for which a steady state necessarily means $v_{18} = 0$. This means that this reaction is at equilibrium with the expected consequence that AMP varies in an opposite direction compared to ATP (Fig. 2a). The simulations confirm this prediction, but show that v_{18} is not necessarily zero between the steady states, making it possible to pass from one steady state value of AMP to one another, i.e.

to modulate v_1 activity. This is particularly the case when the ATPase load is increased with parameter β_{15} (from 1 to 15 in Fig. 3).

2. Entry into the Krebs cycle (v_8) and the Krebs cycle itself (v_9 , v_{10} and v_{11}) appears as a block of reactions (subset), indicating that these reactions will always appear together with the same stoichiometry. In this model, the unique role of the Krebs cycle is to produce $NADH_m$ from pyruvate. Once more the result is obvious when considering the steady state of the differential equations expressing the variations of i_1 , i_2 and c_2 which gives: $v_8 = v_9 = v_{10} = v_{11}$.

The analysis of the 11 elementary modes evidences:

1. Three elementary modes which use the Krebs cycle (efm 8, efm 9 and efm 10; see Table 3 and annexes). All

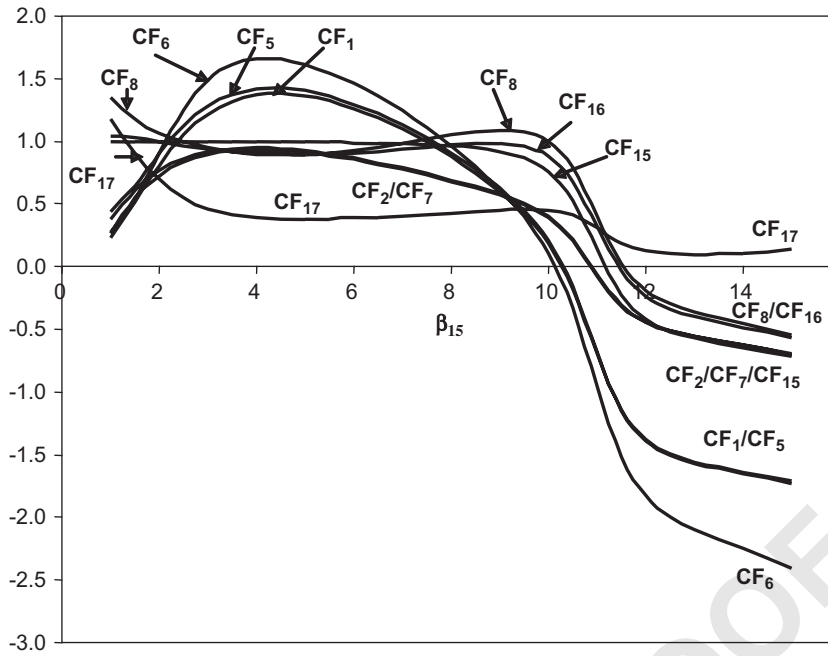


Fig. 4. Variations in some flux control coefficients towards v_{15} as a function of ATPase load β_{15} . The control coefficients are calculated with the same parameters as above. CF_i indicates the control coefficient of the flux through reaction i towards v_{15} , $CF_{v_{15}}^i$.

Table 3
List of the elementary modes

Efm	R ₁	R ₂	R ₃	R ₄	R ₅	R ₆	R ₇	R ₈	R ₉	R ₁₀	R ₁₁	R ₁₂	R ₁₃	R ₁₄	R ₁₅	R ₁₆	R ₁₇	Yield
1	1	1	1	0	1	0	0	0	0	0	0	1	0	1	0	0	0	0
2	1	0	2	0	2	2	0	0	0	0	0	0	2	0	2	0	0	2
3	2	1	3	1	2	2	0	0	0	0	0	0	2	1	0	0	0	0
4	0	0	0	0	0	0	0	0	0	0	0	0	0	0	3	1	1	ind
5	3	3	3	3	0	0	0	0	0	0	0	0	0	3	0	2	2	0
6	1	2	2	2	0	0	2	0	0	0	0	0	0	0	4	2	0	4
7	3	4	4	4	0	0	2	0	0	0	0	0	0	2	0	2	0	0
8	1	2	2	0	2	0	2	2	2	2	2	0	0	0	38	12	0	38
9	1	1	1	0	1	0	0	1	1	1	1	0	0	1	15	5	0	15
10	17	17	17	15	2	0	0	2	2	2	2	0	0	17	0	10	0	0
11	1	2	2	0	2	0	2	0	0	0	0	2	0	0	8	2	0	8

Each row indicates an elementary mode. The number indicates the stoichiometry of the corresponding elementary mode. For instance, the fifth elementary mode is (3 R₁) (3 R₂) (3 R₃) (3 R₄) (3 R₁₄) (2 R₁₆) (2 R₁₇).

correspond to an aerobic glycolysis but one of them (efm 10) produces no ATP ($v_{15} = 0$). In efm 10, the 34 ATP consumed in the first steps of glycolysis are regenerated by the following steps (4 ATP) and by oxidative phosphorylation. The split between v_2 and v_3 results from double constraints to regenerate the $NADH_c$ produced in v_3 and to generate enough $NADH_m$ for the 30 ATP production in mitochondria. The efm 8 corresponds to the aerobic glycolysis described in the textbooks producing 38 ATP per molecule of glucose. The lower yield in ATP production by efm 9 is due to reoxidation of $NADH_c$ without generating an equivalent amount of $NADH_m$. There is a leak in α -GP which does not exist in efm 8.

Table 1 shows that the steady state functioning at

high ATPase load ($\beta_{15} = 10$), i.e. in conditions of large ATP production, does not reach the yield of efm 8. The ATP yield in these conditions is only 10.45 because several leaks occur (through reaction 12 and mainly 13, a lactate leak).

- Other efm's correspond to aerobic glycolysis (involving reaction 16) but do not involve Krebs cycle: efm 5, 6, 7 and 11. Only efm 6 and 11 present a net ATP production.
- Efm 4 is an internal cycle with no glucose entry. It corresponds to production of mitochondrial $NADH_m$ by dehydrogenases (which have to be fed by other respiratory substrates, such as fatty acids). This does not involve the Krebs cycle; there is no efm involving the Krebs cycle without glucose entry.

4. Efm 2 corresponds to purely anaerobic glycolysis with the production of two ATP per glucose molecule.
5. Efm 3 resembles efm 2, except that half of the NADH_c is reduced by cytosolic glycerolphosphate dehydrogenase after splitting of the GAP pool. As a consequence, there is no net ATP production in these conditions.
6. Efm 1 corresponds to anaerobic glycolysis with no ATP production. In this case, NADH_c production is compensated by cytosolic glycerolphosphate dehydrogenase without any involvement of the mitochondria.

6. Discussion

The model studied by Dynnik et al. (1980) was probably one of the first to consider all the components of bioenergetic metabolism including glycolysis, the Krebs cycle and the links between them such as pyruvate dehydrogenase and the NADH shuttle. It also includes the respiratory chain and an ATP consumption reaction which allows the whole system to function.

The simplification of the glycolysis into three parts is logical and has been subsequently adopted by several authors, including Reinhart Heinrich himself. It elegantly separates the ATP-consuming reactions at the beginning from the ATP-synthesizing reactions at the end. In the middle is the oxido-reaction catalysed by the GAP dehydrogenase producing NADH_c , the accumulation of which is a strong constraint on the functioning of glycolysis.

The Krebs cycle is condensed in three linked steps plus the pyruvate dehydrogenase reaction. METATOOL structural analysis clearly shows that these four reactions are what is called “a subset of reactions”, i.e. they are equivalent to only one reaction. This is due to the fact that the intermediate metabolites in the Krebs cycle do not participate in any branched reaction: there is no output or input from/into the Krebs cycle in this model except for the input of pyruvate and the output of NADH_m . In addition, because reactions 8, 10 and 11 are irreversible, the whole Krebs cycle is also irreversible.

The only allosteric regulation involved in the model is the phosphofructokinase (v_1) activation by AMP. This is responsible for the rise in v_1 , and then for most of the fluxes, when β_{15} increases from 1 to 10. However, the “activation” term in the v_1 equation, $(a_1/\mu_0 + \omega)/(a_1/\mu_0 + 1)$, is efficient only for low a_1 (AMP) values due to the low value of μ_0 ($\mu_0 = 0.003$) in the simulations of Dynnik et al. (1980a, b). At very high ATPase load ($\beta_{15} > 10$), there is no longer any AMP regulation on v_1 , so v_1 decreases. In these conditions, one wonders whether a more sophisticated equation of regulation could not be derived for the regulation of v_1 , not only by AMP but also by ATP at a regulatory site (Mazat and Mazat, 1986; Mazat et al., 1977). On the contrary, we can hypothesize that $\beta_{15} = 10$ represents the maximal value of ATP demand in normal

cell conditions, so the v_1 equation is adapted to normal physiological conditions. $\beta_{15} > 10$ would correspond to pathological situations involving a high ATPase load due, for instance, to an enhanced turn-over of a futile cycle consuming high amounts of ATP.

The analysis of the variation of the control coefficients towards v_{15} as a function of β_{15} (Fig. 4) confirms these conclusions. Particularly, the fact that the glycolysis control coefficient ($CF_{v_{15}}^1$ and $CF_{v_{15}}^5$) starts from a low value at $\beta_{15} = 1$ (when the whole network can easily respond to the variations in ATPase load) and rapidly increases with ATP demand to values above 1 is the result of v_1 activation by AMP when the ATP concentration decreases only very slightly. For $\beta_{15} > 5$, v_1 becomes less sensitive to AMP concentration and its control coefficient (and also that of v_5) decreases to reach values of $\beta_{15} = 10$, which are similar to the values of $\beta_{15} = 1$. For higher values of β_{15} ($\beta_{15} > 10$), most of the control coefficients towards v_{15} become negative, expressing the negative effect of an excessive ATPase load.

In the “physiological range” of β_{15} ($\beta_{15} = 1-10$), there are high negative control coefficient values at the branches. This confirms the analysis of Atkinson (1990) who stressed the “properties of enzymes that compete for substrates at branchpoints”. This type of regulation, without an explicit regulator or regulatory mechanism, is responsible for the redistribution of fluxes when ATP consumption increases, with a parallel increase in the “ATP-producing” reactions and a lower relative increase in the leak (the ratio to ATP production v_{15} is decreased).

In this respect, the highly negative effect of an increase in ATPase load on the 1,3-DPG leak (v_4) is particularly pronounced at high ATPase load ($\beta_{15} = 10$). Such an effect is physiologically sensitive because it contributes to the mobilization of more glucose in ATP production. However it is not the consequence of any particular regulation but only the result of the network architecture, particularly the competition occurring at the branchpoints. This is a systemic property of the network.

Importantly, the reactions v_1 and v_{15} have the highest control coefficient on most of the fluxes at steady state. This means that in this metabolic network there is a control by both the supply (v_1) and the demand (v_{15}), illustrating the beginning of a long-standing debate on this subject (Hofmeyr and Cornish-Bowden, 2000). If we consider this metabolic network as an example of a common metabolic network with branches, this result could be of general significance. This shared control is the result of the allosteric regulation on the first step linking the supply to the demand. It also arises from the global response of the network as a whole due to the existence of common substrate pairs (ATP/ADP, NAD/NADH) shared between several reactions. Nevertheless it is possible that supplementary allosteric regulations could change this pattern of control coefficients. For instance, an end-product inhibition of the first reaction would decrease the control coefficients of the supply reaction.

1 This shows the interest of systematically calculating the
control coefficient values.

3 One wonders why Reinhart, who developed with Tom
Rapoport the concept of control coefficient (called in their
5 papers “control strength”; Heinrich and Rapoport, 1973,
1974) at the same time as Kacser and Burns (1973), did not
7 apply this concept in their paper. One reason perhaps is
that the concept was mainly developed for linear pathways
9 (Heinrich and Rapoport, 1973, 1974), and also that the
concept was not largely accepted, or even understood, at
11 that time. Indeed, it must be noticed that at the time of
writing (presumably 1979 or 1978), the first papers of
13 Heinrich and Rapoport had been almost entirely ignored
by the scientific community, and a high proportion of the
15 very few citations were from colleagues in East Germany.
It may be, therefore, that Heinrich did not realize that his
17 papers were to become very well known and thought there
was no point in referring to a concept that appeared to
19 have failed to attract attention.

21 Interestingly, no (glycolytic) oscillations were found in
our simulations, a point which was thoroughly studied by
Sel’kov as early as 1968 (Sel’kov, 1968).

23 The concept of efm was not known in 1980. The
significance of efm analysis is that it points out the
25 structural properties (or even defects) of the network. For
instance, in our case, it appears that reaction 18 is always at
27 equilibrium, which is confirmed by the simulations and the
analysis of the dynamical system. However it should be
29 noted that reaction v_{18} operates in non steady-state
conditions and is responsible for the AMP variations in
31 the transition between the two steady states.

33 The analysis of efm gives the theoretical limits of the
model in terms of ATP production per mole of glucose.
For instance, it demonstrates how far from the theoretical
35 maximal yield a given model with given rate functions may
be. It also shows that this maximal yield cannot be reached
37 if “leak” reactions are operating, thereby sharing the flux
in several efm with different yields.

39 In this model, it is clear that even at high ATP
consumption ($\beta_{15} = 10$), the yield in ATP production does
41 not reach its theoretical maximum due to the leak of
potential ATP producers, mainly pyruvate through lactate.
43 It emphasizes the fact that the metabolism cannot be
oriented entirely to ATP production, because some
45 metabolites are also used in the metabolism (represented
here by the “leak” reactions v_4 , v_{12} , v_{13} and v_{14} in this
47 network). This is also well known for the Krebs cycle,
although it is not taken into account in Fig. 1.

49 The paper was probably the first attempt at modelling
the whole cellular energetic metabolism. At that time, it
51 provided an explanation for the Pasteur effect presented in
the following paper (Heinrich et al., 1980a, b) based on
53 “the interrelationship of glycolysis, the Krebs cycle and H-
transporting shuttles at varying rates of oxidative phos-
55 phosphorylation and ATPase load”.

57 Such a model is ideal to understand how the flux of ATP
production is split between glycolysis and oxidative

phosphorylation and the interrelationship between the
various parts of the network for ATP production and
59 NADH_c reoxidation. It should be pointed out that the
articulating role of the H-transporting shuttles, although
61 essential, is not always considered in the more recent
models.

63 As it is, this paper is certainly a good starting point for
developing more complex models. Conversely, as a
65 minimal model, it can help in understanding some basic
features of more complex metabolic networks such as the
67 flux modulations resulting from the branched structure of
the network itself and the articulation between the large
69 blocks of the energetic metabolism, in order to balance
what is called the metabolite currencies (ATP, NADH,
71 etc.) in different steady states.

73 Uncited references Q3

75 Cornish-Bowden and Cárdenas (1990) and Duarte et al.
(2007).

77 Acknowledgements

79 We thank Vitalii Selivanov (University of Barcelona)
and Sergei Petrovskii (University of Leicester) for their
81 help. We are indebted to Ivan Chang and Ray Cooke for
revising the English. This work was supported by ACI
83 IMPBio.

85 Appendix A. Supplementary Materials

87 Supplementary data associated with this article can be
found in the online version at [doi:10.1016/
91 j.jtbi.2008.01.003](https://doi.org/10.1016/j.jtbi.2008.01.003).

93 References

- 95 Atkinson, D.E., 1990. What should a theory of metabolic control offer to
97 the experimenter? In: Cornish-Bowden, A., Cárdenas, M.L. (Eds.),
Control of Metabolic Processes. Plenum Press, New York, pp. 3–11.
99 Cornish-Bowden, A., Cárdenas, M.-L., 1990. Control of Metabolic
Processes. Plenum Press. 101
103 Duarte, N.C., Becker, S.A., Jamshidi, N., Ines Thiele, I., Mo, M.L., Thuy,
D., Vo, T.D., Srivas, R., Bernhard Palsson, B.Ø., 2007. Global
reconstruction of the human metabolic network based on genomic and
105 bibliomic data. PNAS 104, 1777–1782.
107 Dynnik, V.V., Heinrich, R., Sel’kov, E.E., 1980a. A mathematical model
of carbohydrate energy metabolism. Interaction between glycolysis,
the Krebs cycle and the H-transporting shuttles at varying ATPases
load. Biokhimiya 45, 771–782 (in Russian).
109 Dynnik, V.V., Heinrich, R., Sel’kov, Ye.Ye., 1980b. A mathematical
model of carbohydrate energy metabolism. Interaction glycolysis, the
Krebs cycle, and the H-transporting shuttles at varying ATPase load.
111 Biochemistry (New York) 45 (5), 589–598 (in English).
113 Heinrich, R., Rapoport, T.A., 1973. A linear steady-state treatment of
enzymatic chains: its application for the analysis of the crossover
theorem and of the glycolysis of human erythrocytes. Acta Biol. Med.
Ger. 31, 479–494.

- 1 Heinrich, R., Rapoport, T.A., 1974. A linear steady-state treatment of
enzymatic chains. General properties, control and effector strength.
3 Eur. J. Biochem. 42, 89–95.
- 5 Heinrich, R., Dynnik, V.V., Sel'kov, E.E., 1980a. Mathematical model for
carbohydrate energy metabolism. Mechanism of the Pasteur effect.
7 Biokhimiya 45, 963–973 (in Russian).
- 9 Heinrich, R., Dynnik, V.V., Sel'kov, Ye.Ye., 1980b. A mathematical
model for carbohydrate energy metabolism. The mechanism of the
Pasteur effect. Biochemistry (New York) 45 (6), 731–738 (in English).
- 11 Hofmeyr, J.-H.S., Cornish-Bowden, A., 2000. Regulating the cellular
economy of supply and demand. FEBS Lett. 476, 47–51.
- 13 Kacser, H., Burns, J.A., 1973. The control of flux. Symp. Soc. Exp. Biol.
32, 65–104.
- 15 Mazat, J.-P., Mazat, F., 1986. Double site enzyme and squatting: where
one regulatory ligand is also a substrate of the reaction. J. Theor. Biol.
121, 89–103.
- Mazat, J.-P., Langla, J., Mazat, F., 1977. Double site enzyme and
squatting. J. Theor. Biol. 68, 365–383.
- Pfeiffer, T., Sanchez-Valdenebro, I., Nuno, J.C., Montero, F., Schuster,
S., 1999. Metatool: for studying metabolic networks. Bioinformatics
15, 251–257.
- Schuster, S., Hilgetag, C., 1994. On elementary flux modes in biochemical
reaction systems at steady state. J. Biol. Syst. 2, 165–182.
- Schuster, S., Dandekar, T., Fell, D.A., 1999. Detection of elementary
modes in biochemical networks: a promising tool for pathway analysis
and metabolic engineering. Trends Biotechnol. 17, 53–60.
- Schuster, S., Fell, D.A., Dandekar, T., 2000. A general definition of
metabolic pathways useful for systematic organization and analysis of
complex metabolic networks. Nat. Biotechnol. 18, 326–332.
- Sel'kov, E.E., 1968. Self-oscillations in glycolysis. Eur. J. Biochem. 4,
79–86.

UNCORRECTED PROOF